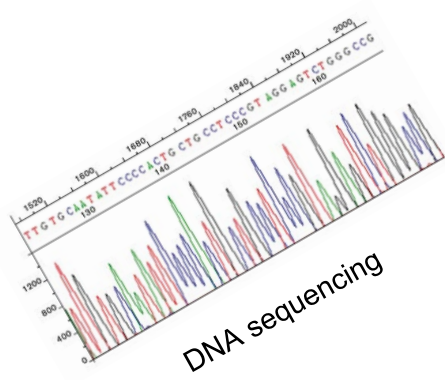


# Interpretable multimodal deep learning for brain imaging and genomics data integration

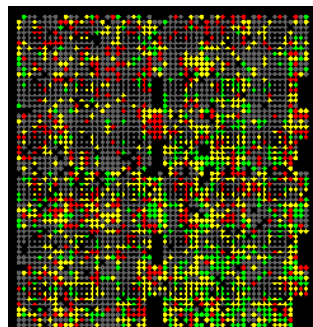
Yu-Ping Wang

Biomedical Engineering,  
Biostatistics and Data Science  
Computer Science, & Neurosciences  
Tulane University  
Email: wyp@tulane.edu

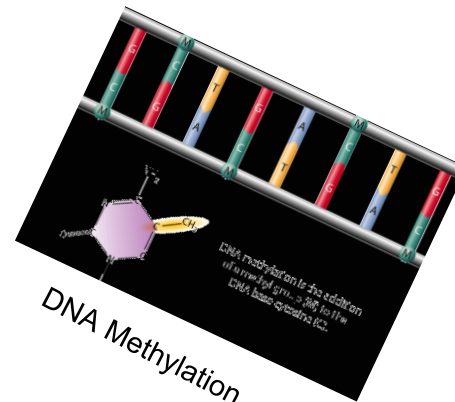
# Multiscale and multimodal data fusion



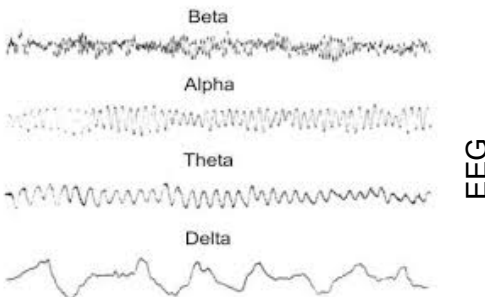
DNA sequencing



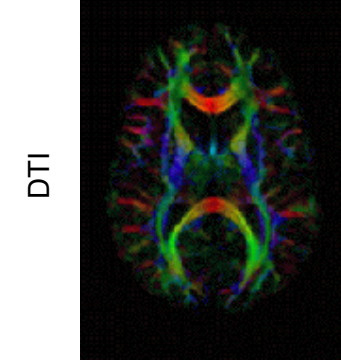
Gene expression



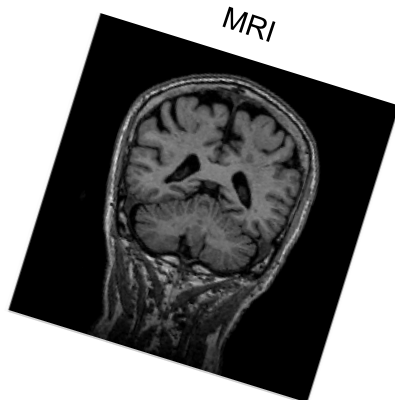
DNA Methylation



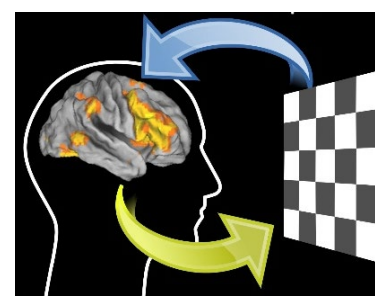
EEG



DTI

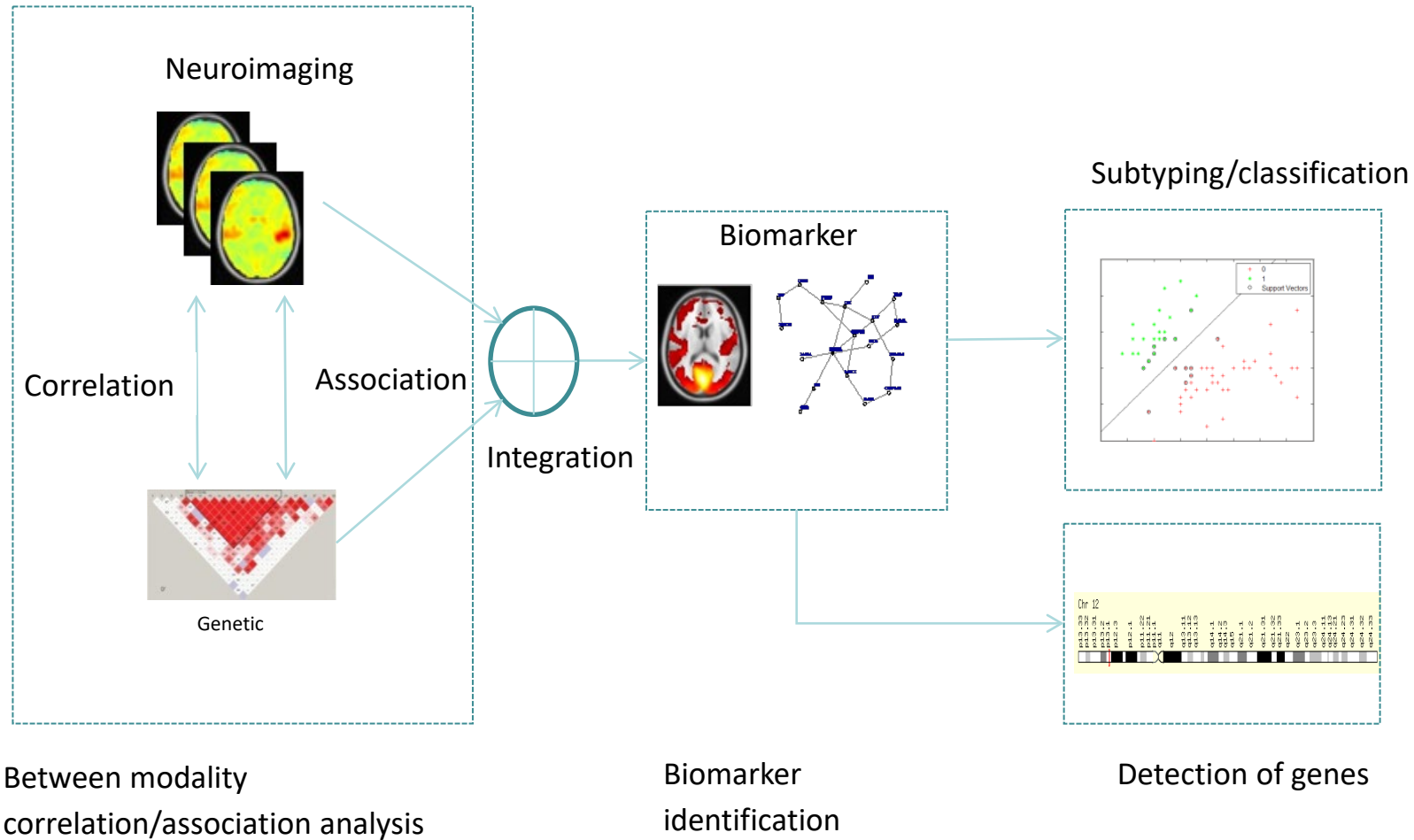


MR/



fMRI

# A framework for imaging and genomics data integration



# Challenges for big imaging and genomics data fusion

- **Multi-scale and modal data**  
sMRI, rsfMRI, tfMRI, SNPs, methylation, ....
- **Multiple types of data**  
continuous, discrete, binary, ...
- **Model development**
  - Linear (e.g., ICA, CCA, sparse regression ) vs non-linear (e.g., kernel CCA, distance correlation, deep networks)
  - Two way correlation (e.g., CCA) vs multi-way correlation (e.g., mCCA, tensor decomposition)
  - two view fusion (e.g., gICA) vs multi-view fusion (e.g., multi-task learning, NMF, graphical models)

# Multidisciplinary approaches

- 1. Development of sophisticated mathematical models**
  - Multiple and kernel CCA models
  - Projected distance correlation
  - Multiple graphical models
  - Multi-view learning combining regression and correlation
  - Graphical Fourier transform
  - Tensor decomposition
  - Alternative diffusion maps
  - Deep learning fusion of structure/function
  - Time varying graphical LASSO model
  - Causality modeling with Bayesian approach
  - .....
- 2. Cross-validate with both public and in house data sets**
- 3. Translate into clinical and medical use with multidisciplinary approach**

# Canonical Correlation Analysis (CCA) model

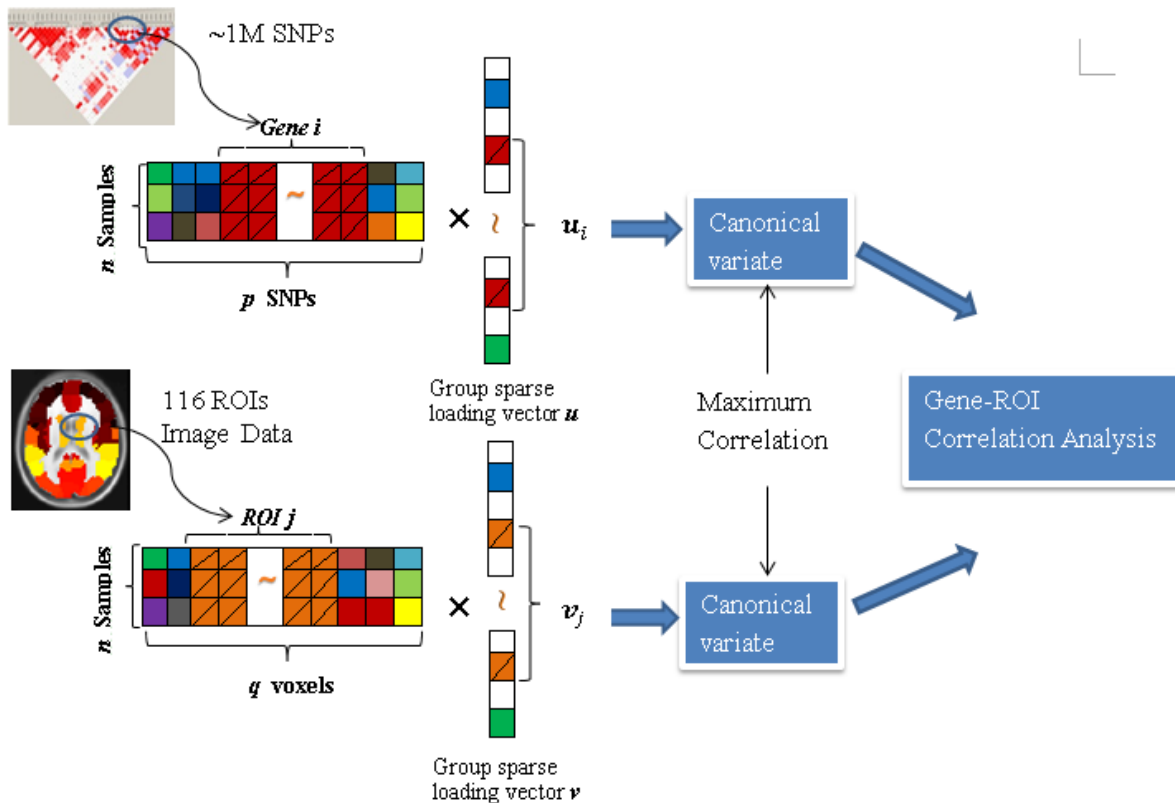


Illustration of combining both imaging and SNP data with the CCA model to identify correlated genes and ROIs.

# Canonical correlation analysis (CCA)

(Hotelling, H. (1936))

Input:  $X_1 \in \mathbb{R}^{n \times r}, X_2 \in \mathbb{R}^{n \times s}$

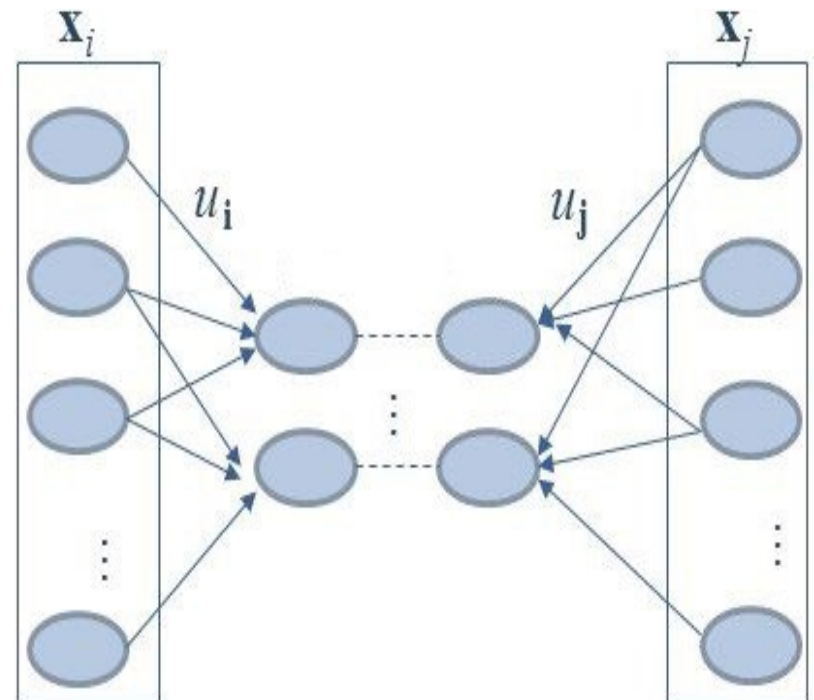
To optimize

$$(u_1^*, u_2^*) = \underset{u_1, u_2}{\operatorname{argmax}} u_1' \Sigma_{12} u_2$$

subject to  $u_1' \Sigma_{11} u_1 = u_2' \Sigma_{22} u_2 = 1$

where  $u_1 \in \mathbb{R}^{r \times 1}, u_2 \in \mathbb{R}^{s \times 1}, \Sigma_{ij} := X_i' X_j$

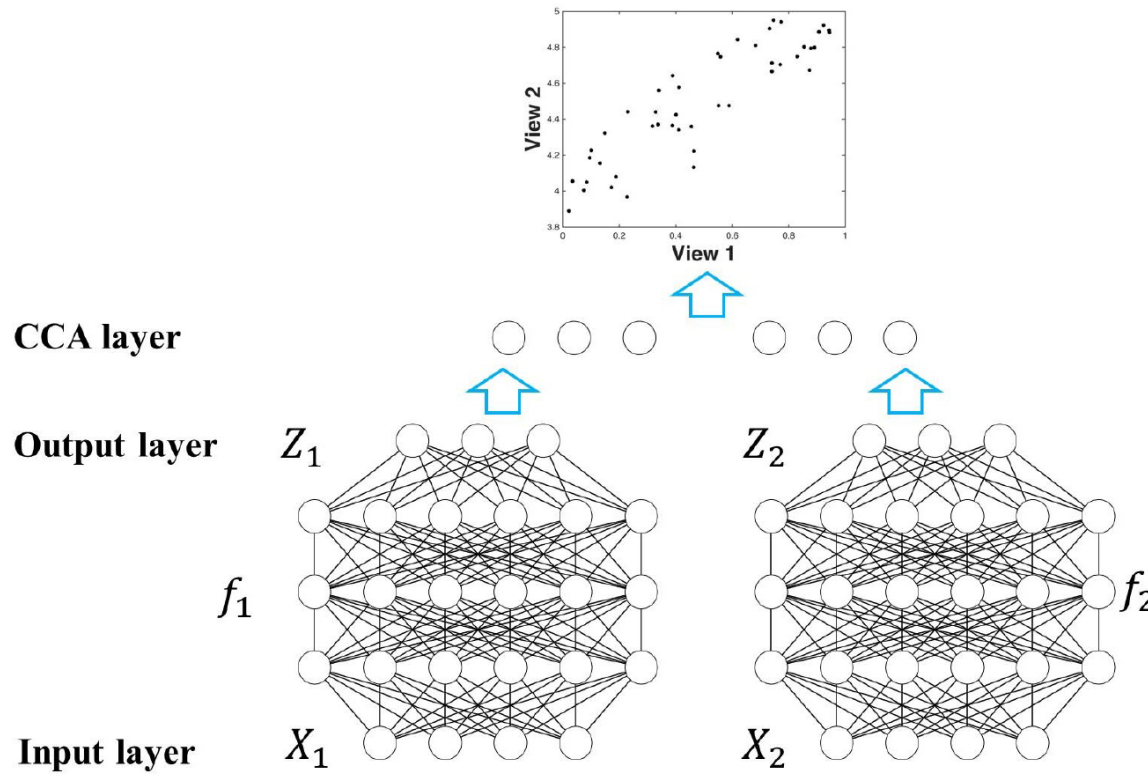
- Detects cross-data correlations
- Dimension reduction
- Unable to do biomarker selection



**CCA can detect the correlation between multiple datasets  
but cannot link with phenotypes!**

# Deep CCA

(Andrew et al. @ICML13', Wang et al. @ICML15')



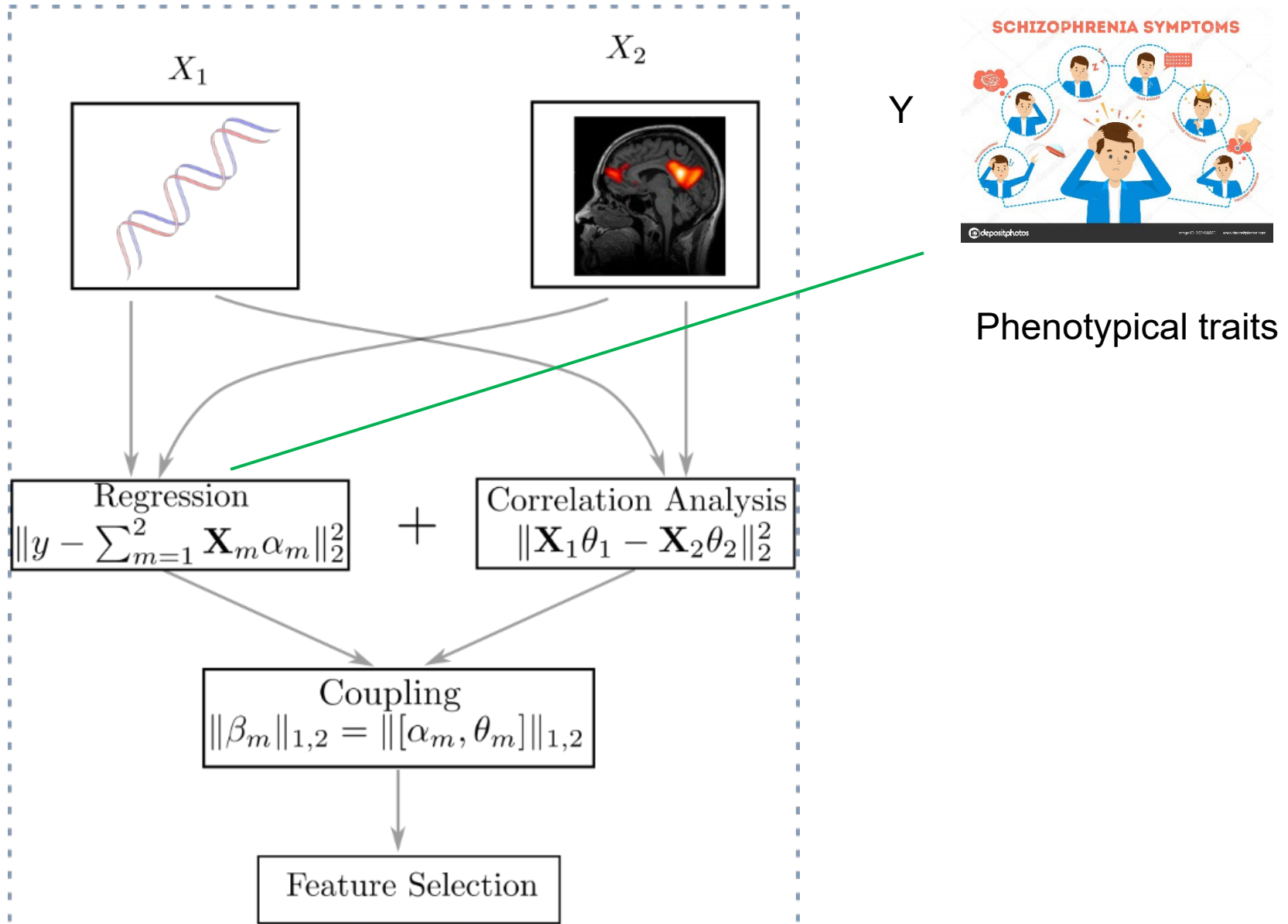
## Pros

- Network representation
- More flexible to detect complex correlations

## Cons

- The identified associations are not trait/label related (limited biomedical impact).

# Co-regularized learning: *regression + correlation*



# Collaborative regression (CR)

(SM. Cross & R. Tibshirani, 2014)

Input:  $X_1 \in \mathbb{R}^{n \times r}, X_2 \in \mathbb{R}^{n \times s}$ , label data  $Y \in \mathbb{R}^{n \times 1}$

To optimize

$$(u_1^*, u_2^*) = \operatorname{argmin}_{u_1, u_2} b_1 \|X_2 u_2 - X_1 u_1\|_2 + b_2 \|Y - X_1 u_1\|_2 + b_3 \|Y - X_2 u_2\|_2$$

## Pros

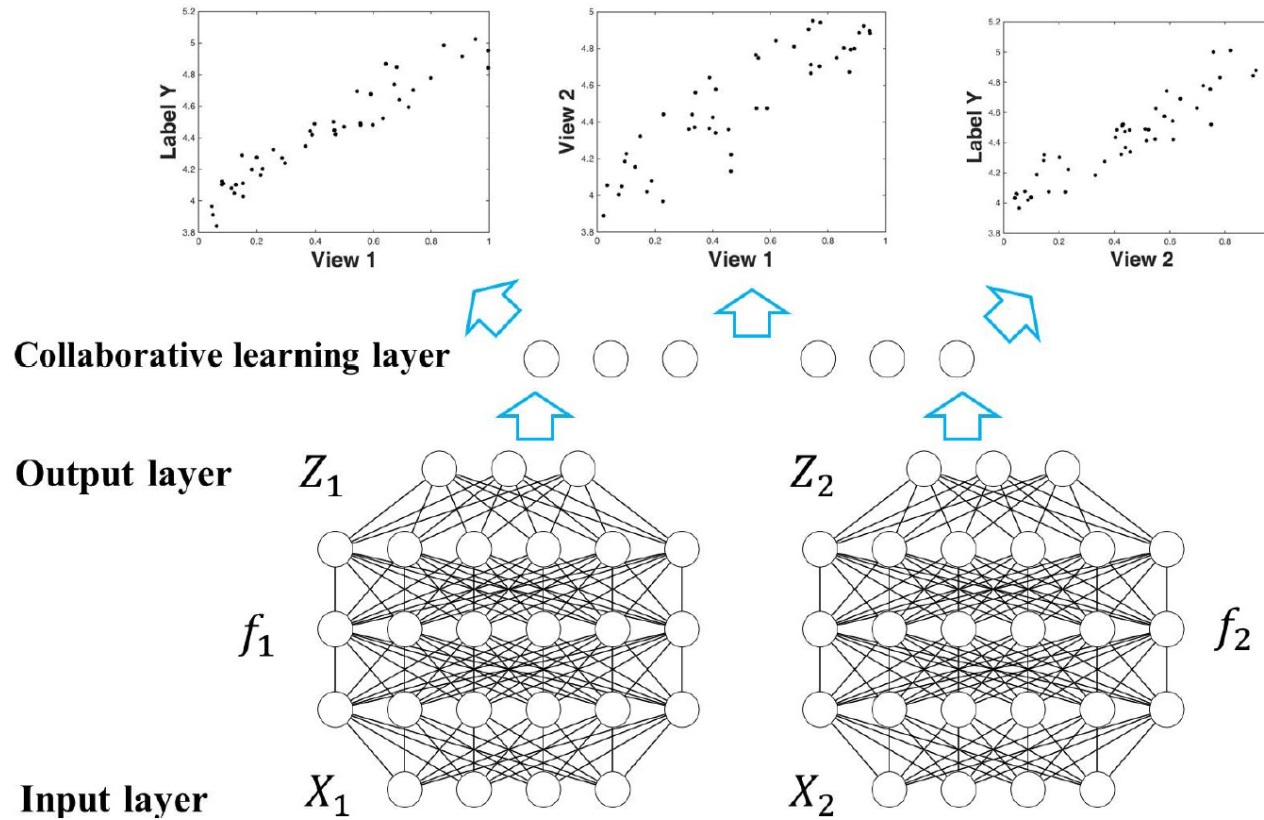
- Incorporates regression into CCA
- Detects label/trait related correlations

## Cons

- Unable to capture complex relationships

Pascal Zille, Vince D. Calhoun, Yu-Ping Wang, [Enforcing Co-expression Within a Brain-Imaging Genomics Regression Framework](#), IEEE Transactions on Medical Imaging, 28 June 2017, Page(s): 1-1, DOI: 10.1109/TMI.2017.2721301, PMID: 28678703

# Deep collaborative learning (DCL)



- Combine correlation analysis and regression using deep network representations
- More flexible to detect complex cross-omics associations
- Improved performance on both correlation detection and prediction due to the network representation and the combination of regression and correlation

# Formulation of Deep collaborative learning (DCL)

## Objective function

$$\begin{aligned}(Z_1^*, Z_2^*) &= \operatorname{argmax}_{Z_1, Z_2} \left\{ \max_{U_1, U_2} \operatorname{Trace}(U_1' Z_1' Z_2 U_2) - \min_{\beta_1} \|Y - Z_1 \beta_1\|_2^2 \right. \\ &\quad \left. - \min_{\beta_2} \|Y - Z_2 \beta_2\|_2^2 \right\} \\ &= \operatorname{argmax}_{Z_1, Z_2} \left\{ \|\Sigma_{11}^{-\frac{1}{2}} \Sigma_{12} \Sigma_{22}^{-\frac{1}{2}}\|_{tr} - \|Y - Z_1 (Z_1' Z_1)^{-1} Z_1' Y\|_2^2 \right. \\ &\quad \left. - \|Y - Z_2 (Z_2' Z_2)^{-1} Z_2' Y\|_2^2 \right\}\end{aligned}$$

subject to  $U_1' \Sigma_{11} U_1 = U_2' \Sigma_{22} U_2 = I$

where  $Z_1 = f_1(X_1)$ ,  $Z_2 = f_2(X_2)$ ,  $\Sigma_{ij} = Z_i' Z_j$

$f_1, f_2$  are two deep networks

and  $\|A\|_{tr} := \operatorname{Trace}(\sqrt{A' A}) = \sum \sigma_i$

# Deep collaborative learning (Gradient)

- Mini-batch stochastic gradient descent (mini-batch SGD) is used to train DCL's network; and back-propagation (BP) is used to pass the gradient from one layer to another layer.
- To apply mini-batch SGD and BP, the gradient of DCL's objective function is needed.

## DCL's Gradient

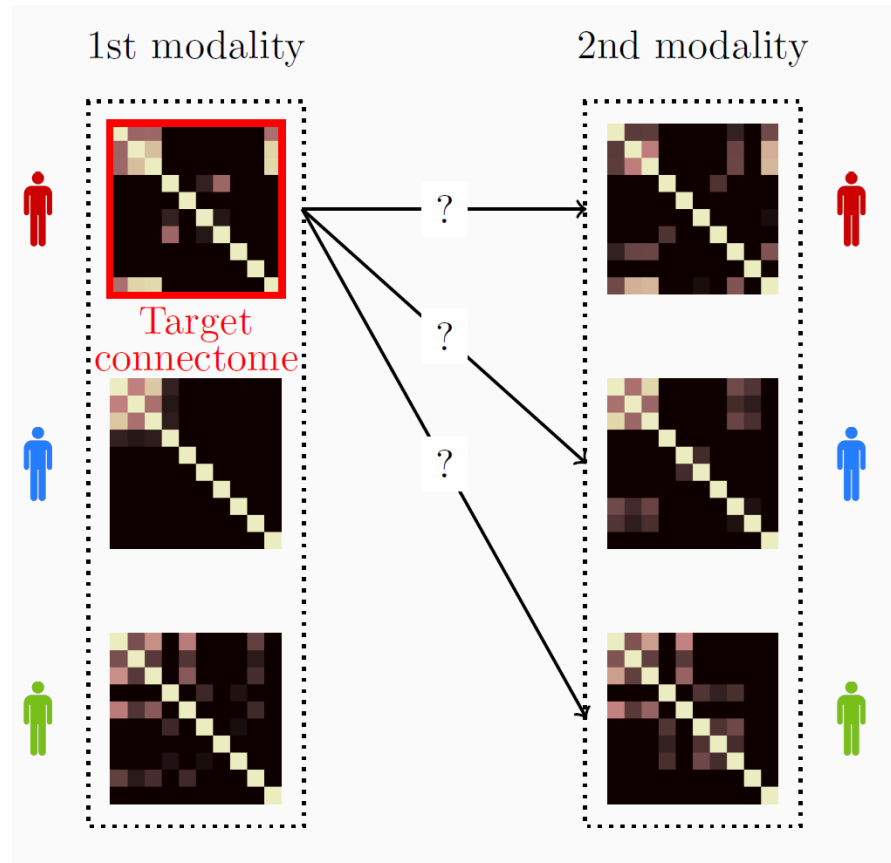
$$\begin{aligned}\frac{\partial \text{Obj.Fun}}{\partial Z_1} = & -Z_1 \Sigma_{11}^{-\frac{1}{2}} UDU^T \Sigma_{11}^{-\frac{1}{2}} + Z_2 \Sigma_{22}^{-\frac{1}{2}} VU^T \Sigma_{11}^{-\frac{1}{2}} \\ & + 2YY^T Z_1 (Z_1^T Z_1)^{-1} - 2Z_1 (Z_1^T Z_1)^{-1} Z_1^T YY^T Z_1 (Z_1^T Z_1)^{-1}\end{aligned}$$

$$\begin{aligned}\frac{\partial \text{Obj.Fun}}{\partial Z_2} = & -Z_2 \Sigma_{22}^{-\frac{1}{2}} VDV^T \Sigma_{22}^{-\frac{1}{2}} + Z_1 \Sigma_{11}^{-\frac{1}{2}} UV^T \Sigma_{22}^{-\frac{1}{2}} \\ & + 2YY^T Z_2 (Z_2^T Z_2)^{-1} - 2Z_2 (Z_2^T Z_2)^{-1} Z_2^T YY^T Z_2 (Z_2^T Z_2)^{-1}\end{aligned}$$

where  $[U, D, V] = \text{svd}(\Sigma_{11}^{-\frac{1}{2}} \Sigma_{12} \Sigma_{22}^{-\frac{1}{2}})$

# Brain connectivity networks as fingerprints

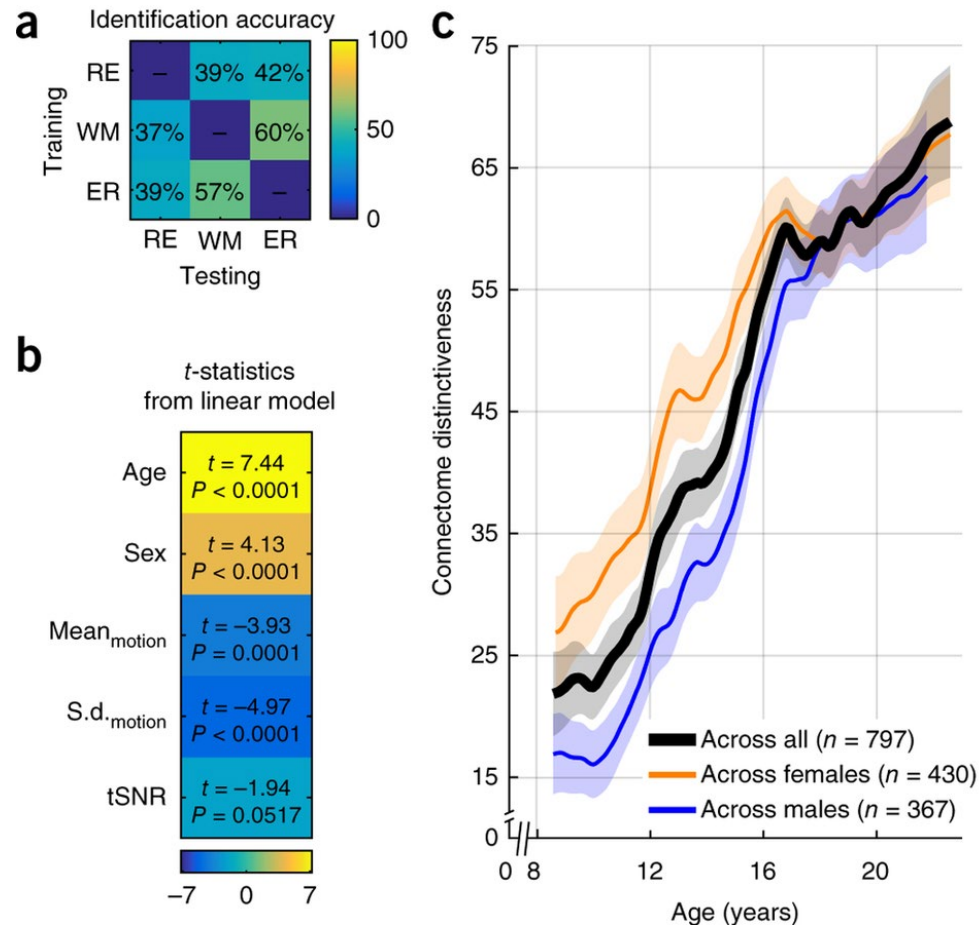
- Functional connectivity profiles act as a fingerprint that can accurately identify subjects from a large group
- It can also predict fluid intelligence



*Finn et al., Functional connectome fingerprinting: identifying individuals using patterns of brain connectivity, Nature Neuroscience, 2015.*

# Brain connectome and age

- Functional connectome develops into an individual wiring pattern through adolescence
- The brain functional connectome is more distinct with increasing age.
- It also differs between genders.



Kaufmann et al. “Delayed stabilization and individualization in connectome development are related to psychiatric disorders.” Nature Neuroscience 2017

# Real data analysis - Data

Philadelphia Neurodevelopmental Cohort (PNC)

Subjects: 989 adolescents (age 8-22)

rest fMRI

Resting state  
fMRI; 124 time  
points

nback fMRI

Memory task  
fMRI; 231 time  
points

emoid fMRI

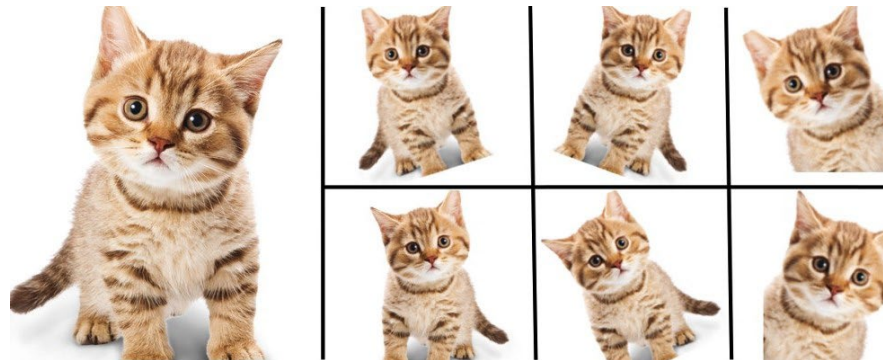
Emotion task  
fMRI; 210 time  
points

Preprocessed (motion correction, spatial normalization, spatial smoothing) using SPM

Run deep collaborative learning on each combination: rest-nback;  
rest-emoid; nback-emoid.

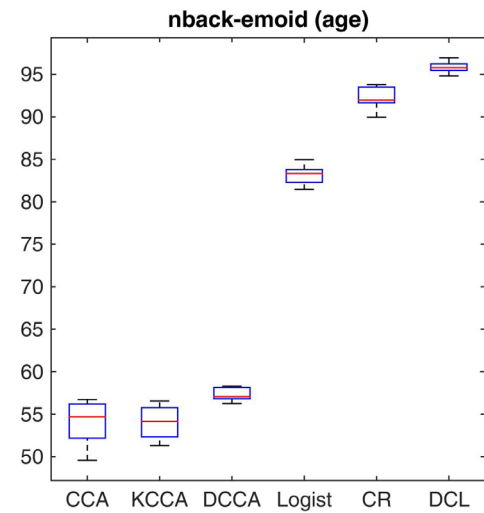
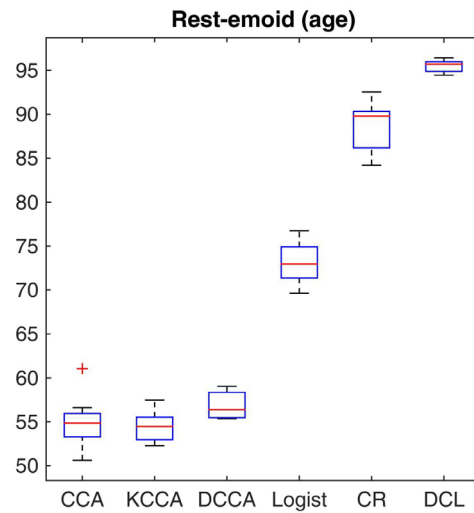
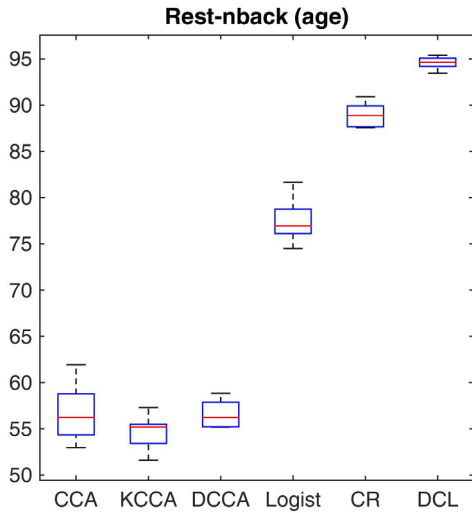
# Data augmentation

- Training deep network requires a large sample size.
- Data augmentation is a popular technique in image processing fields, which conducts reasonable transformation (such as image rotation, reflection, scaling) on raw images.



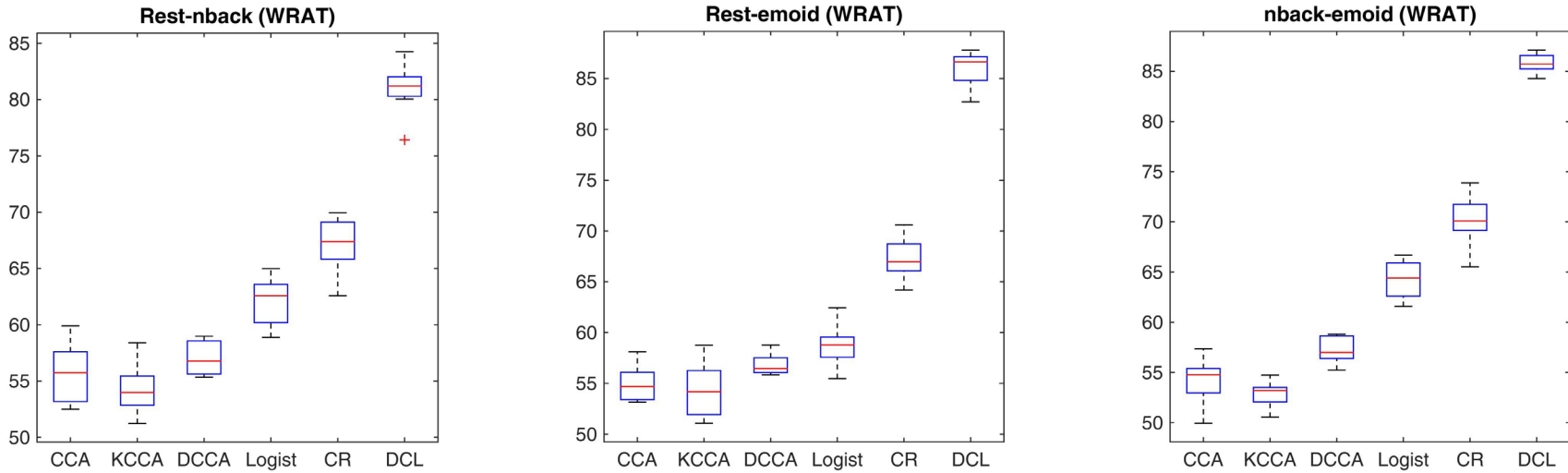
- Brain connectivity reflects the correlation between different voxels/ROIs across a series of time points.
- We generated more samples by re-sampling in the temporal space (with time window length > 60 secs) (Leonardi 2015);
- Training set and testing set were separated before augmentation.

# Classifying age groups



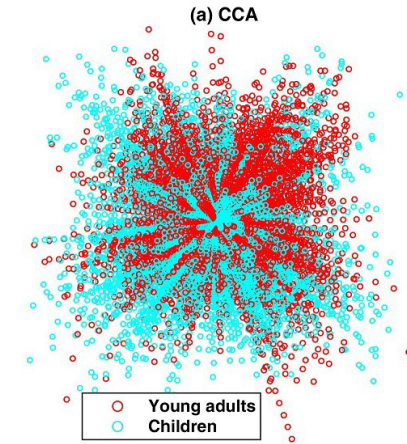
- Methods for comparison:  
CCA, kernel CCA, Deep CCA, Logistic regression,  
Collaborative regression (CR), Deep collaborative learning (DCL)
- Age groups: Preteens (8-11 years) and young adults (18-22 years)

# Classifying groups of different Intelligent Quotient (IQ) : Wide Range Achievement Test (WRAT)

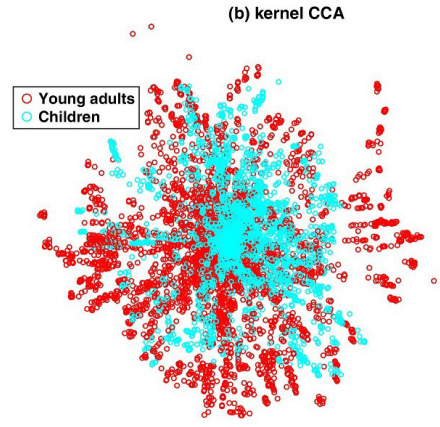


- IQ/WRAT groups: low WRAT group (score 55-89) and high WRAT group (score 114-145).
- Compared to deep CCA, deep collaborative learning yields much higher classification accuracies.
- Brain connectivities perform better in classifying age groups than in classifying cognition abilities.

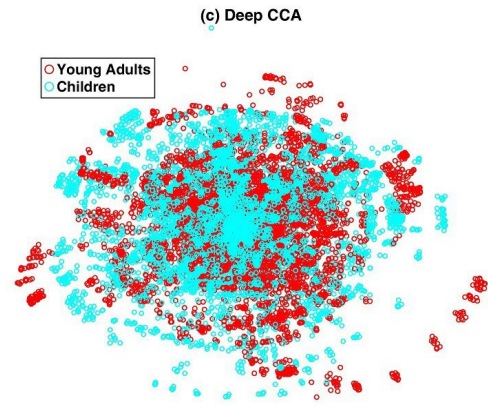
# Visualization of different data representations



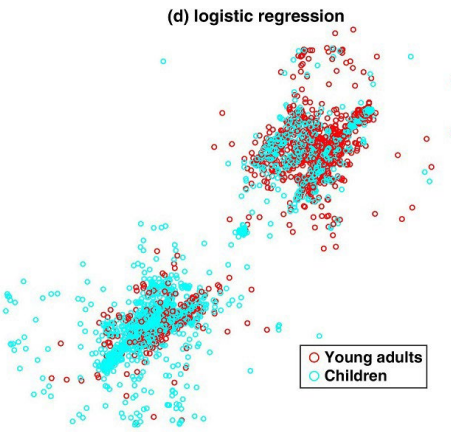
(a) CCA



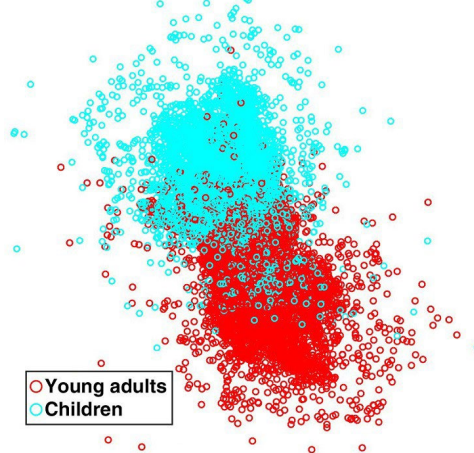
(b) Kernel CCA



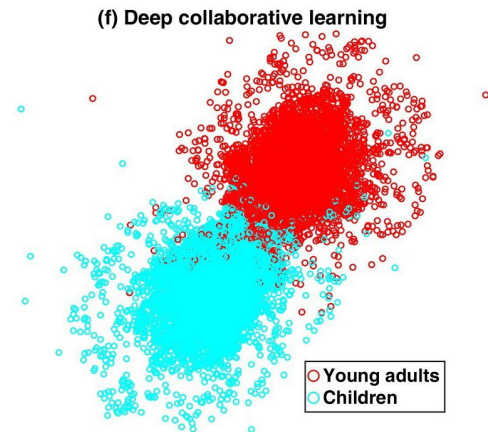
(c) Deep CCA



(d) Logistic regression



(e) Collab regression



(f) Deep CL

# Interpretation of identified brain subnetwork

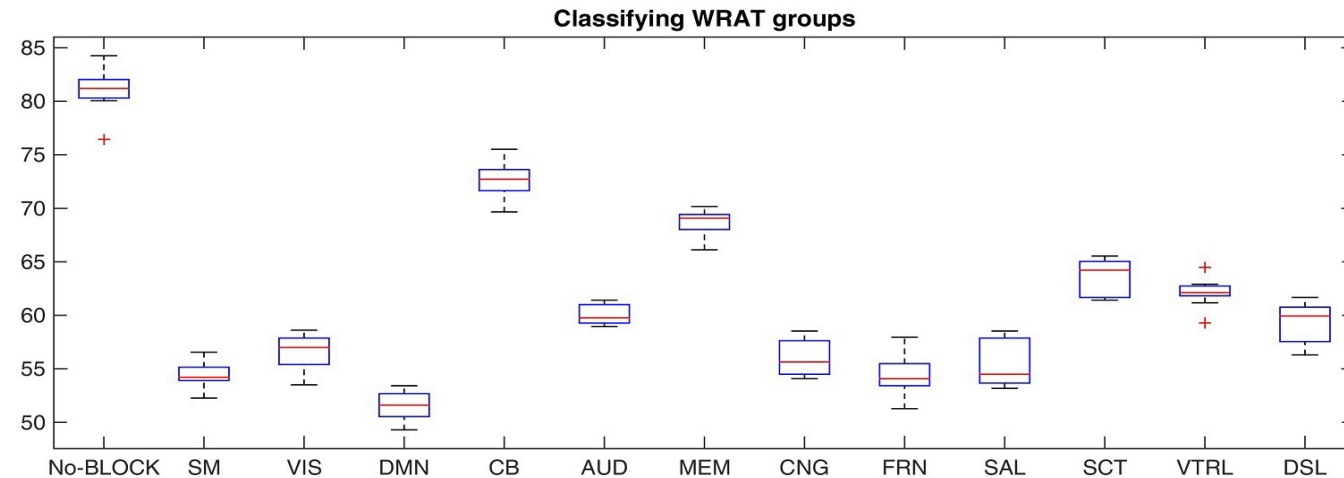
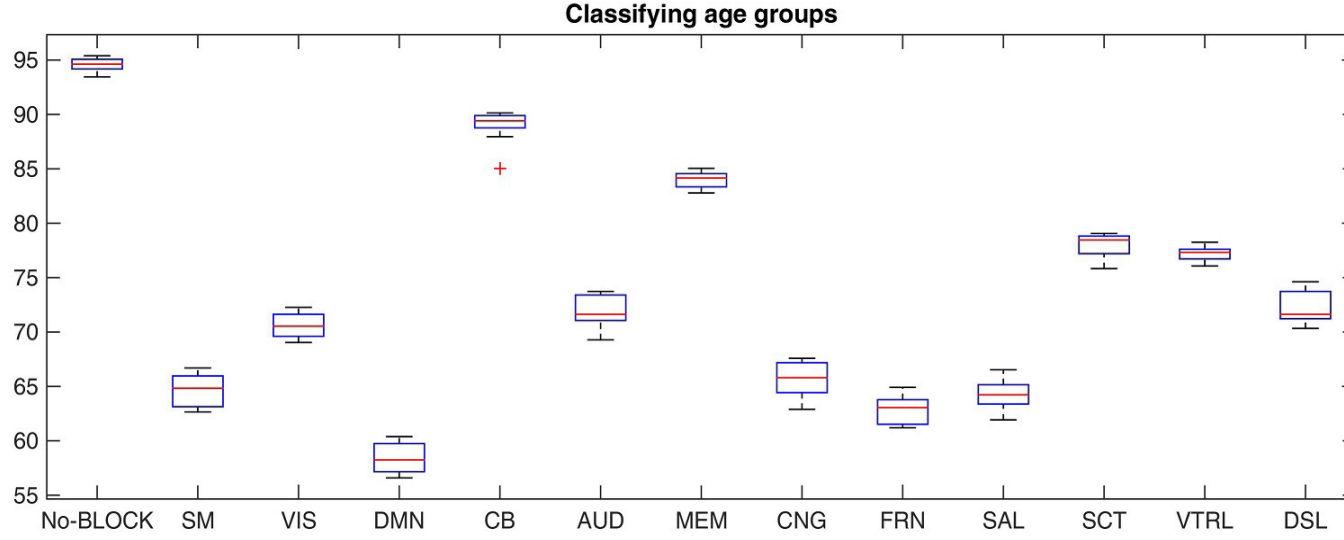
Since deep network is a black box, it is not able to provide p-values for further ROI analysis.

To investigate the discriminative power of each brain intrinsic network in classifying age groups or cognition groups, we occlude each brain sub-network individually and test if the classification accuracy drops.

## Brain sub-networks

sensorimotor network (SM), visual network (VIS), default mode network (DMN), cerebellum (CB), auditory network (AUD), memory retrieval network (MEM), cingulo-opercular task control (CNG), salience network (SAL), subcortical network (SCT), ventral attention (VTRL), dorsal attention (DSL)

# Identification of brain subnetwork using occlusion sensitivity (OS) analysis



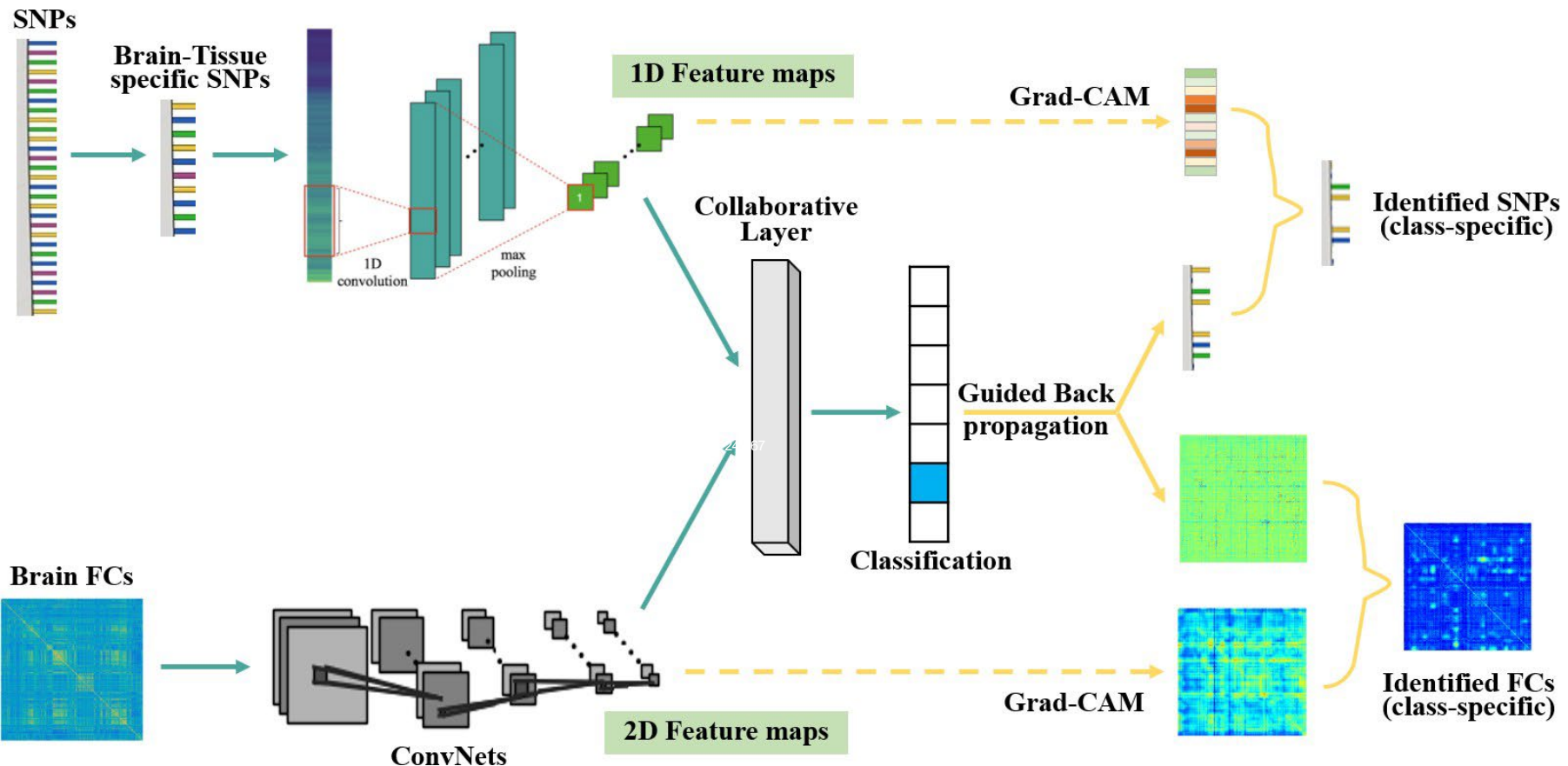
# Further information

Wenxing Hu, Biao Cai, Aiying Zhang, Vince D. Calhoun, Yu-Ping Wang, [Deep collaborative learning with application to multimodal brain development study](#), IEEE Transactions on Biomedical Engineering,  
Date of Publication: 13 March 2019; DOI:  
10.1109/TBME.2019.2904301



Wenxing Hu, PhD

# Grad-CAM guided convolutional collaborative learning (gCAM-CCL)



- The obtained activation maps quantify pixel-level contributions of the input features.
- This is achieved by combining intermediate feature maps using gradient-based weights.
- Class-specific activation maps (CAM) further facilitate biological mechanism analysis.

# How to fuse two networks: collaborative layer

- The collaborative learning layer<sup>1</sup> in our deep collaborative learning (DCL) model considers both cross-data associations and their fittings to the class labels.
- In our earlier work<sup>1</sup> on DCL, the loss function was dependent on the batch size, leading to a problem for model training.
- In this model, we use a batch-size-independent loss function.

## Loss function

### Two classes scenario

$$\text{Loss} = - \sum_{i=1}^2 \left( (1-y) \log(h_1^{(i)}) + y \log(1-h_2^{(i)}) \right) - \sum_{i=1}^2 \left( h_i^{(1)} \log(h_i^{(2)}) + h_i^{(2)} \log(h_i^{(1)}) \right)$$

where  $h_i^{(1)}$ ,  $h_i^{(2)}$  are the outputs of two ConvNets,  $y$  represents class label.

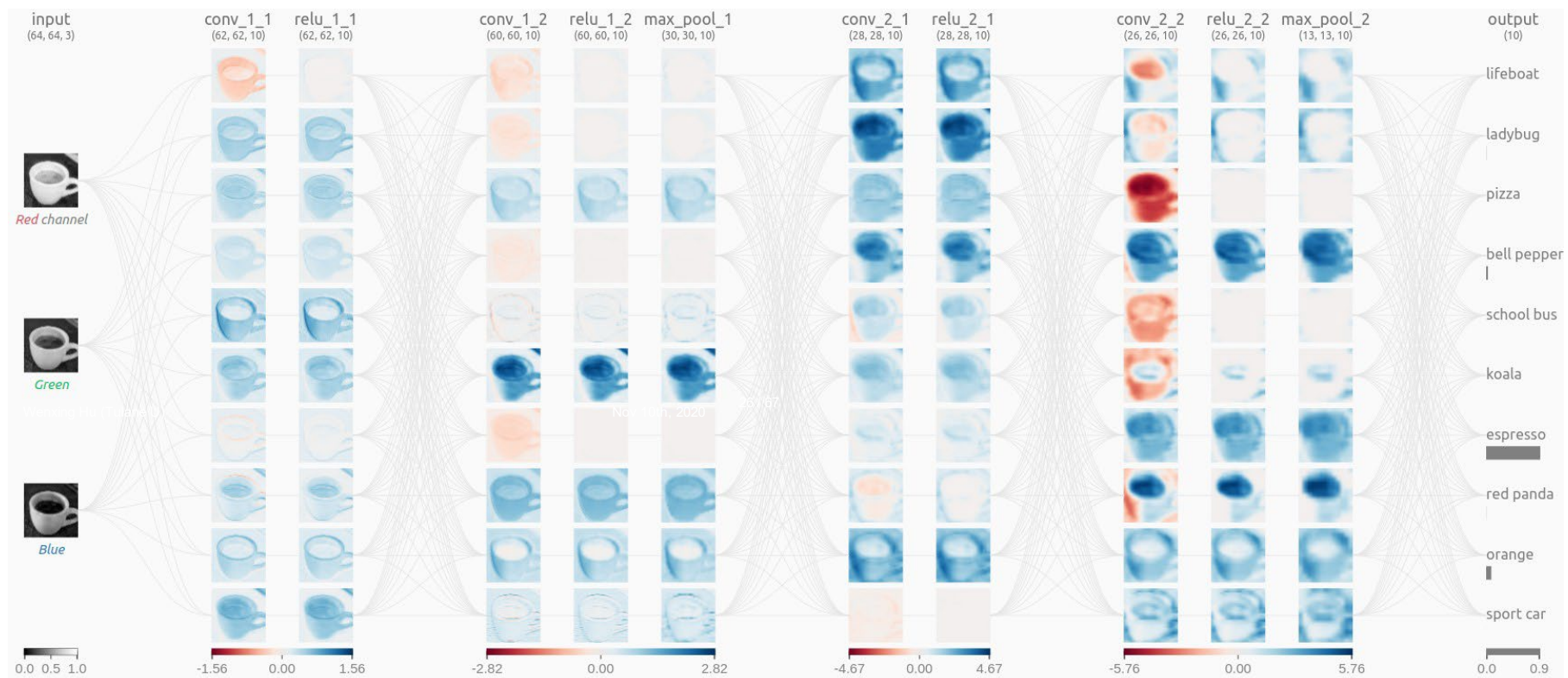
### Multiple classes scenario

$$\text{Loss} = - \frac{1}{m} \sum_{i=1}^m \sum_{c=1}^C y_c \log(h_c^{(i)}) - \frac{1}{m(m-1)} \sum_{i,j(i \neq j)}^m \sum_{c=1}^C h_c^{(i)} \log(h_c^{(j)})$$

where  $m$  represents the number of views,  $C$  represents the number of classes, and  $y_c$  represents the class label for class  $c$ .

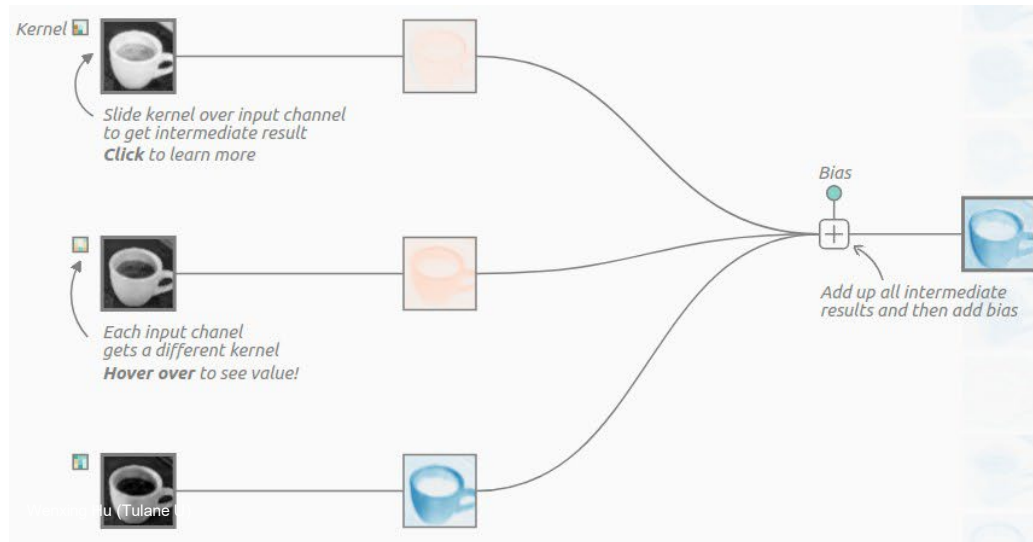
*Hu, Wenzing, et al. "Deep collaborative learning with application to the study of multimodal brain development." IEEE TBME (2019).*

# How to interpret CNN: An example of CNN



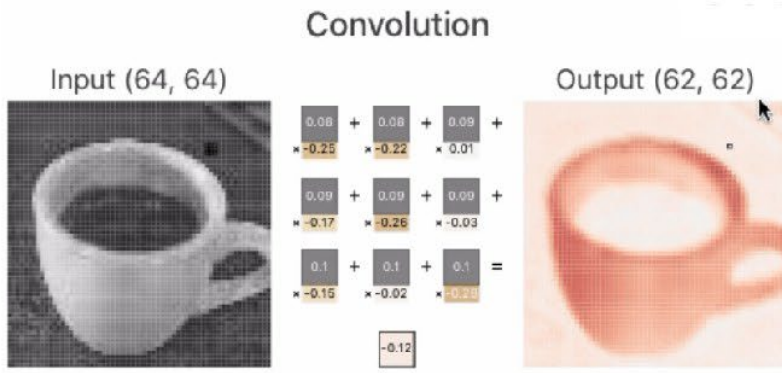
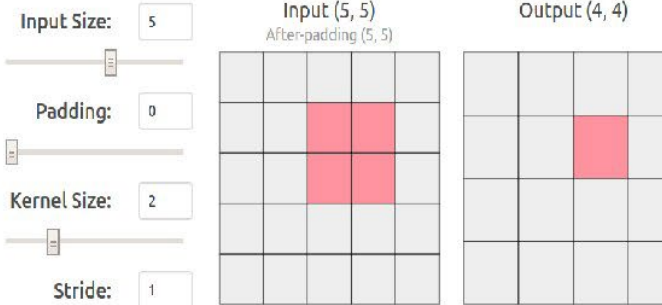
<https://poloclub.github.io/cnn-explainer>

# How to interpret CNN: CNN is complicated

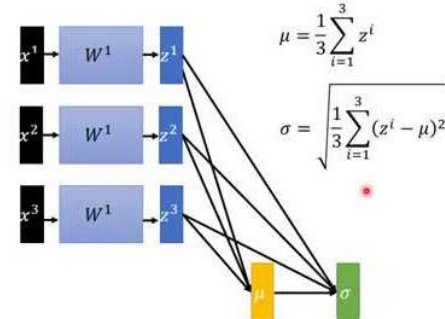


$$\text{ReLU}(x) = \max(0, x)$$

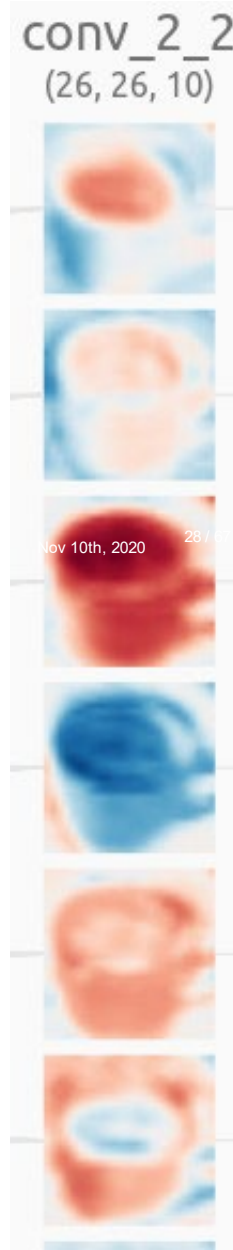
$$\text{Softmax}(x_i) = \frac{\exp(x_i)}{\sum_j \exp(x_j)}$$



Batch normalization

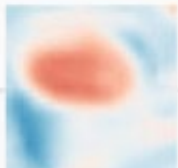


# How to interpret CNN: feature maps

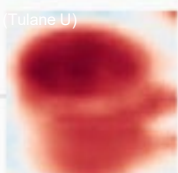


# How to combine feature maps

conv\_2\_2  
(26, 26, 10)



Tulane U



- In order to combine feature maps, a set of weights are needed.
- Some methods, i.e., CAM (class activation maps), calculates the weights by retraining the deep network: add an additional classification layer after the feature-map-layer.
  - 1. Not end-to-end;
  - 2. Needs extra training (time consuming);
  - 3. classification accuracy drops due to the break of original architecture.

# How to interpret CNN: Grad-CAM and Guided Back-Propagation (BP)

## Grad-CAM: class-specific; interpreting high-level feature maps

The formulations of how Grad-CAM calculates weights  $g_k^c$  and activation maps  $\text{map}_{\text{gradcam}}$  are as follows.

$$g_k^c = \text{global\_avg\_pooling}\left(\frac{\partial y^c}{\partial F^k}\right)$$

where  $y^c$  represents the prediction score for class  $c$ ,  $F^k$  represents the  $k$ th feature map, and

$$\text{map}_{\text{gradcam}} = \text{upsampling}\left(\sum_{k=1}^K g_k^c F^k\right)$$

## Guided BP: high resolution; interpreting raw image inputs

$$\frac{\partial L}{\partial h^l} = \llbracket (h^l > 0) \& \& (h^{l+1} > 0) \rrbracket$$
  
$$\frac{\partial L}{\partial h^{l+1}}$$

Backward pass:  
*guided  
backpropagation*

0	0	0
6	0	0
0	0	3

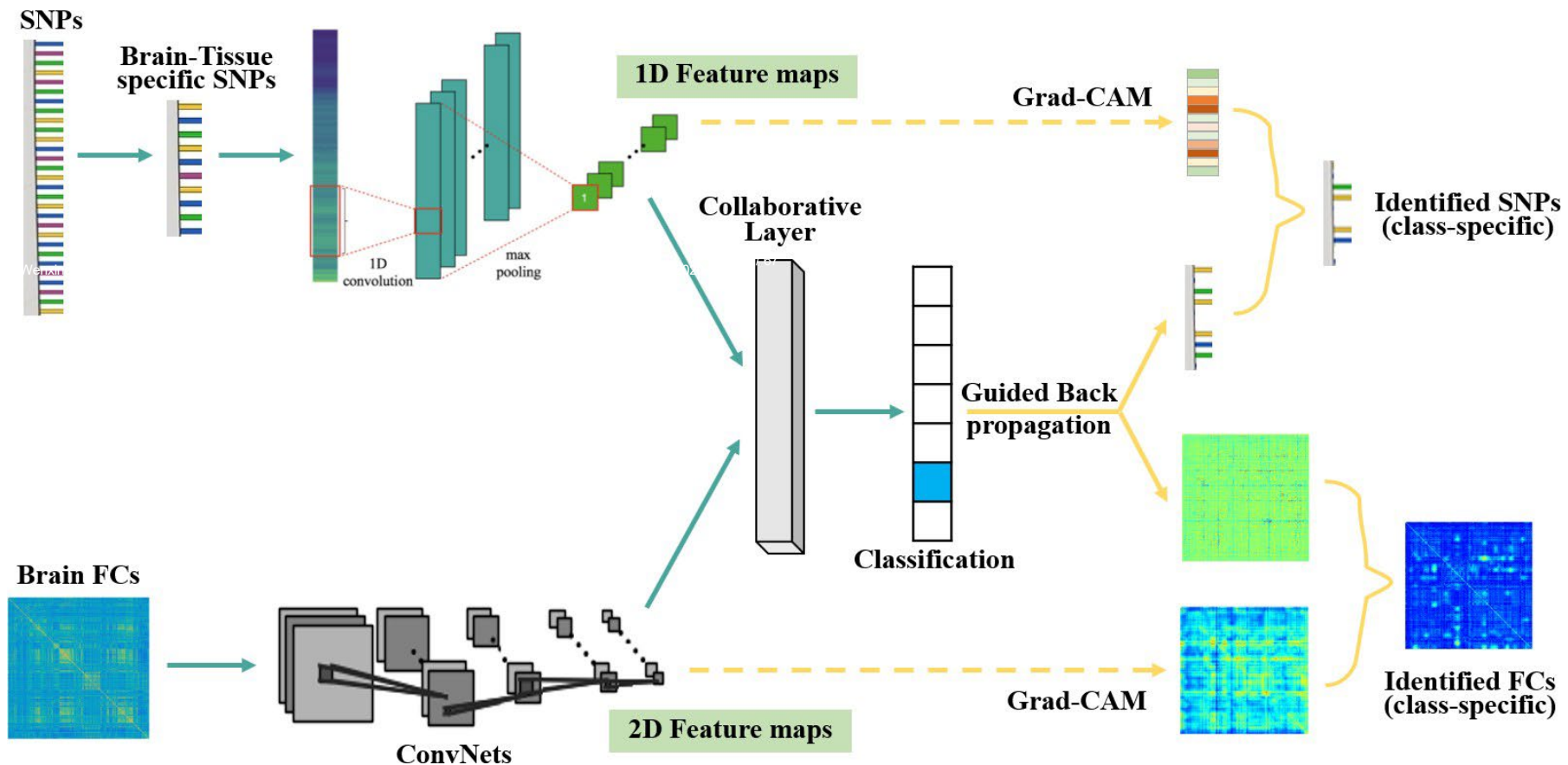
-2	3	-1
6	-3	1
2	-1	3

$$\frac{\partial L}{\partial h^{l+1}}$$



# Our Model: Grad-CAM guided convolutional collaborative learning (gCAM-CCL)

- Grad-CAM: class-specific activation maps
- Guided BP: high resolution activation maps



# Application to a brain cognition study - PNC cohort

Philadelphia Neurodevelopmental Cohort (PNC)

Subjects: 854 adolescents (aged 8-21 years)

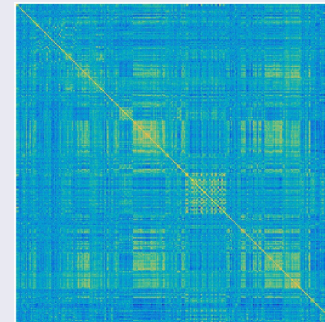
## SNPs

Brain tissue specific (based on GTEx<sup>1</sup>)

Brain amygdala	Brain nucleus accumbens
Brain caudate	Brain cerebellar hemisphere
Brain cerebellum	Brain frontal cortex
Brain cortex	Brain substantia nigra
Brain putamen	Brain anterior cingulate cortex
Brain spinal cord	Brain hypothalamus
Brain hippocampus	

## nback fMRI

Memory task fMRI; 264\*264 functional connectivity matrix



1. Genotype-Tissue Expression (GTEx) <https://www.gtexportol.org/home/>

# Application to a brain cognition study - PNC cohort

## Philadelphia Neurodevelopmental Cohort (PNC)

Subjects: 854 adolescents (aged 8-21 years)

- The wide range achievement test (WRAT) score, a measure of comprehensive cognitive ability, including reading, comprehension, math skills, etc., was used to evaluate the cognitive ability of each subject.
- Two classes: low WRAT group (the bottom 20% group WRAT 55-89) versus high WRAT group (the top 20% group WRAT 114-145).
- training set (70%), validation set (15%), and test set (15%).

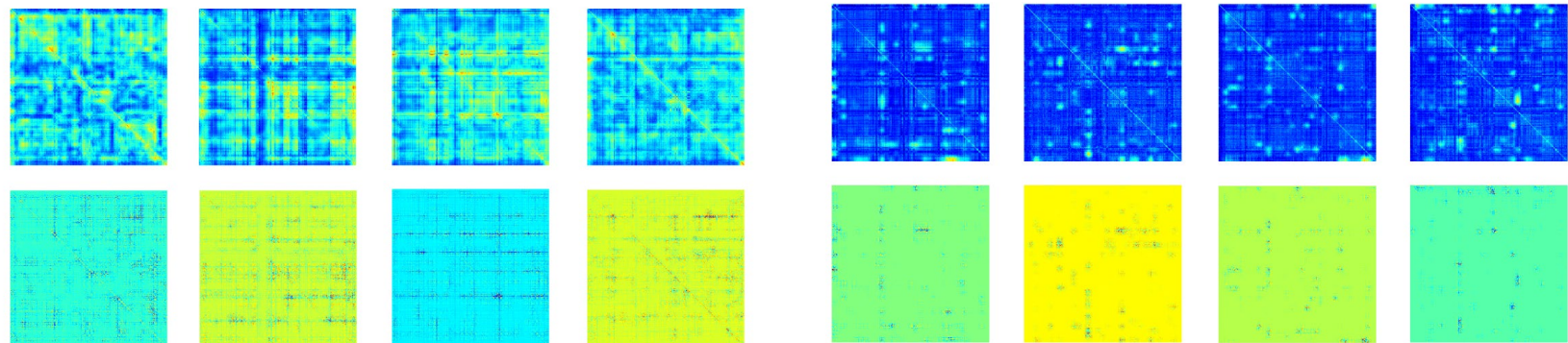
# WRAT classification results

Table: The comparison of classification performances (Low/High WRAT classification).

Classifier	ACC	SEN	SPF	F1
gCAM-CCL	0.7501	0.7762	0.7157	0.7610
CCL+SVM	0.7387	0.7637	0.7083	0.7504
CCL+RF	0.7419	0.7666	0.7014	0.7523
MLP	0.7231	0.7555	0.6915	0.7215
SVM	0.7082	0.7562	0.6785	0.7093
DT	0.6626	0.6778	0.6430	0.6605
RF	0.7119	0.7559	0.6714	0.7138
Logist	0.6745	0.7386	0.6285	0.6900

The brain FC activation maps for low and High WRAT group.

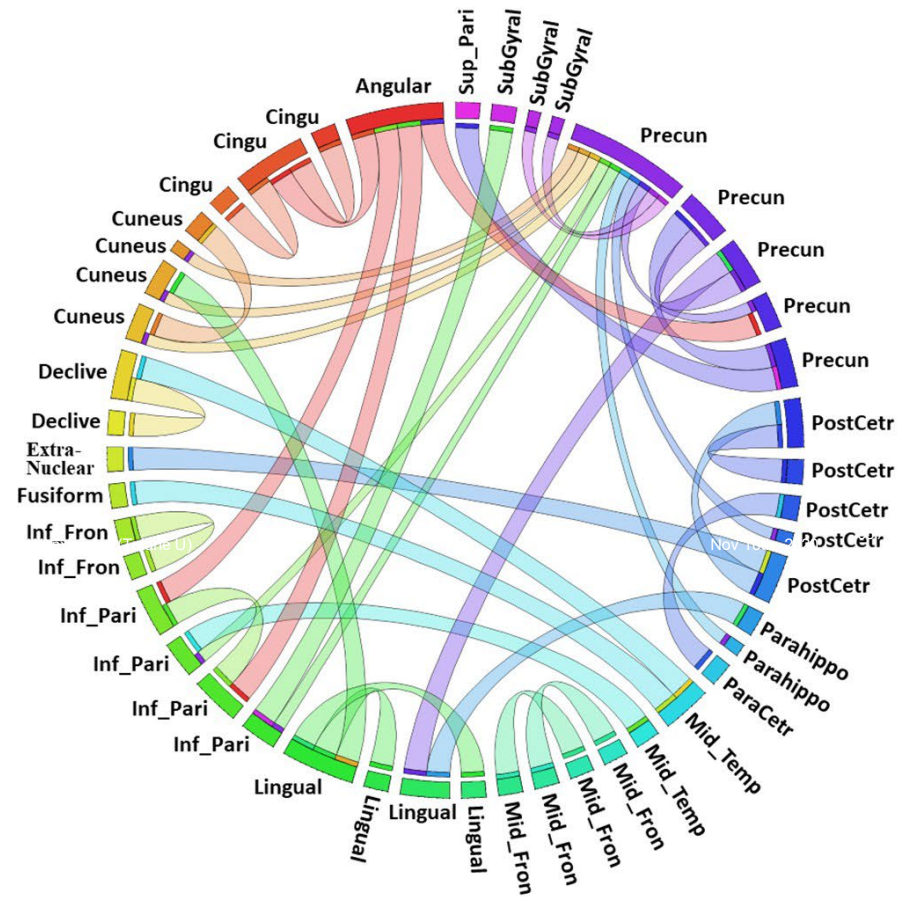
Grad-CAM (top 4 subfigures) and Gradient-Guided Grad-CAM (bottom 4 subfigures).



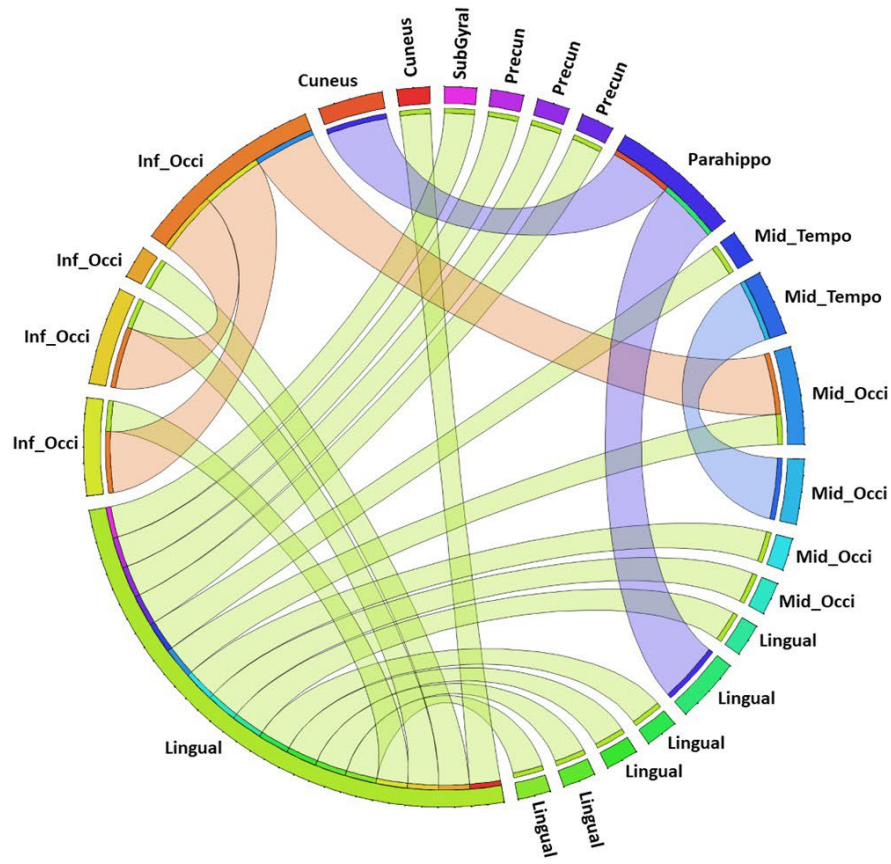
Low WRAT group

High WRAT group

# Identified Brain functional connectivities (FCs)



(a) Low WRAT group



(b) High WRAT group

The length of a circle arc indicates the number of ROI-ROI connections on this ROI.

Three hub ROIs (lingual, middle and inferior occipital): visual processing, object recognition, and word processing.

# Identified genes

TABLE V: Identified SNP loci (Low WRAT group)

SNP rs #	Gene	SNP rs #	Gene
rs1642763	ATP1B2	rs997349	MTURN
rs9508	ATPIF1	rs17547430	MTURN
rs2242415	BASP1	rs7780166	MTURN
rs11133892	BASP1	rs10488088	MTURN
rs10113	CALM3	rs3750089	MTURN
rs11136000	CLU	rs2275007	OSGEP
rs4963126	DEAF1	rs4849179	PAX8
rs11755449	EEF1A1	rs11539202	PDHX
rs2073465	EEF1A1	rs1045288	PSMD13
rs1809148	EEF1D	rs7563960	RNASEH1
rs4984683	FBXL16	rs145290	RP1
rs7026635	FBXW2	rs446227	RP1
rs734138	FLYWCH1	rs414352	RP1
rs2289681	GFAP	rs6507920	RPL17
rs7258864	GNG7	rs12484030	RPL3
rs4807291	GNG7	rs10902222	RPLP2
rs887030	GNG7	rs8079544	TP53
rs7254861	GNG7	rs6726169	TTL
rs12985186	GNG7	rs415430	WNT3
rs2070937	HP	rs8078073	YWHAE
rs622082	IGHMBP2	rs12452627	YWHAE
rs12460	LINS	rs324126	ZNF880
rs10044354	LNPEP		

TABLE VI: Identified SNP loci (High WRAT group)

SNP rs #	Gene	SNP rs #	Gene
rs3787620	APP	rs1056680	MB
rs373521	APP	rs9257936	MOG
rs2829973	APP	rs7660424	MRFAP1
rs1783016	APP	rs3802577	PHYH
rs440666	APP	rs1414396	PHYH
rs2753267	ATP1A2	rs1414395	PHYH
rs10494336	ATP1A2	rs1037680	PKM
rs1642763	ATP1B2	rs2329884	PPM1F
rs10113	CALM3	rs1045288	PSMD13
rs2053053	CAMK2A	rs2271882	RAB3A
rs4958456	CAMK2A	rs12294045	SLC1A2
rs4958445	CAMK2A	rs3794089	SLC1A2
rs3756577	CAMK2A	rs7102331	SLC1A2
rs874083	CAMK2A	rs3798174	SLC22A1
rs3011928	CAMTA1	rs9457843	SLC22A1
rs890736	CPLX2	rs1443844	SLC22A1
rs17065524	CPLX2	rs6077693	SNAP25
rs12325282	FAHD1	rs363043	SNAP25
rs104664	FAM118A	rs362569	SNAP25
rs6874	FAM69B	rs10514299	TMEM161B-AS1
rs7026635	FBXW2	rs4717678	TYW1B
rs12735664	GLUL	rs8078073	YWHAE
rs7155973	HSP90AA1	rs10521111	YWHAE
rs2251110	LOC101928134	rs4790082	YWHAE
rs2900856	LOC441242	rs10401135	ZNF559
rs8136867	MAPK1		

# Gene enrichment analysis

TABLE VII: Gene enrichment analysis of the identified genes (Low WRAT group). Q-values represent multiple testing corrected p-value.

Pathway Name	Pathway Source	Set size	Contained	p-value	q-value
Eukaryotic Translation Elongation	Reactome	106	5	1.18E-06	1.65E-05
Peptide chain elongation	Reactome	101	4	3.12E-05	2.18E-04
Calcium Regulation in the Cardiac Cell	Wikipathways	149	4	1.48E-04	6.89E-04
Translation	Reactome	310	5	2.09E-04	7.33E-04
Metabolism of proteins	Reactome	2008	11	3.96E-04	1.11E-03
Midbrain development	Gene Ontology	94	4	1.22E-05	1.53E-03
Site of polarized growth	Gene Ontology	167	4	1.25E-04	2.19E-03
Growth cone	Gene Ontology	165	4	1.20E-04	4.07E-03
Cellular catabolic process	Gene Ontology	2260	12	7.22E-05	4.55E-03
Pathways in cancer - Homo sapiens (human)	KEGG	526	5	2.39E-03	5.58E-03
Metabolism of amino acids and derivatives	Reactome	342	4	3.20E-03	6.40E-03

TABLE VIII: Gene enrichment analysis of the identified genes (High WRAT group). Q-values represent multiple testing corrected p-value.

Pathway Name	Pathway Source	Set size	Contained	p-value	q-value
Regulation of neurotransmitter levels	Gene Ontology	335	9	6.77E-10	1.04E-07
Transmission across Chemical Synapses	Reactome	224	7	7.75E-08	2.40E-06
Synaptic signaling	Gene Ontology	711	10	3.17E-08	2.43E-06
Insulin secretion - Homo sapiens (human)	KEGG	85	5	3.26E-07	5.06E-06
Organelle localization by membrane tethering	Gene Ontology	170	6	1.34E-07	6.84E-06
Regulation of synaptic plasticity	Gene Ontology	179	6	1.89E-07	7.21E-06
Exocytosis	Gene Ontology	909	10	3.06E-07	9.36E-06
Membrane docking	Gene Ontology	179	6	1.82E-07	1.28E-05
Vesicle docking involved in exocytosis	Gene Ontology	45	4	5.11E-07	1.30E-05
Plasma membrane bounded cell projection part	Gene Ontology	1452	12	3.05E-07	1.34E-05
Cell projection part	Gene Ontology	1452	12	3.05E-07	1.37E-05
Neurotransmitter release cycle	Reactome	51	4	1.76E-06	1.37E-05
Synaptic Vesicle Pathway	Wikipathways	51	4	1.76E-06	1.37E-05
Neuronal System	Reactome	368	7	2.25E-06	1.39E-05
Secretion by cell	Gene Ontology	1493	12	4.13E-07	1.45E-05
Adrenergic signaling in cardiomyocytes - Homo sapiens (human)	KEGG	144	5	4.47E-06	2.31E-05
Gastric acid secretion - Homo sapiens (human)	KEGG	75	4	8.34E-06	3.70E-05
Neuron part	Gene Ontology	1713	12	1.83E-06	4.09E-05
Plasma membrane bounded cell projection	Gene Ontology	2098	13	2.22E-06	4.87E-05

## More information

Wenxing Hu, Xianghe Meng, Yuntong Bai, Aiying Zhang, Gang Qu, Biao Cai, Gemeng Zhang, Tony W. Wilson, Julia M. Stephen, Vince D. Calhoun, Yu-Ping Wang, Interpretable multimodal fusion networks reveal mechanisms of brain cognition, IEEE Transactions on Medical Imaging, Page(s):1-1, Date of Publication: February 08 2021; DOI: 10.1109/TMI.2021.3057635



Wenxing Hu, PhD

# Summary

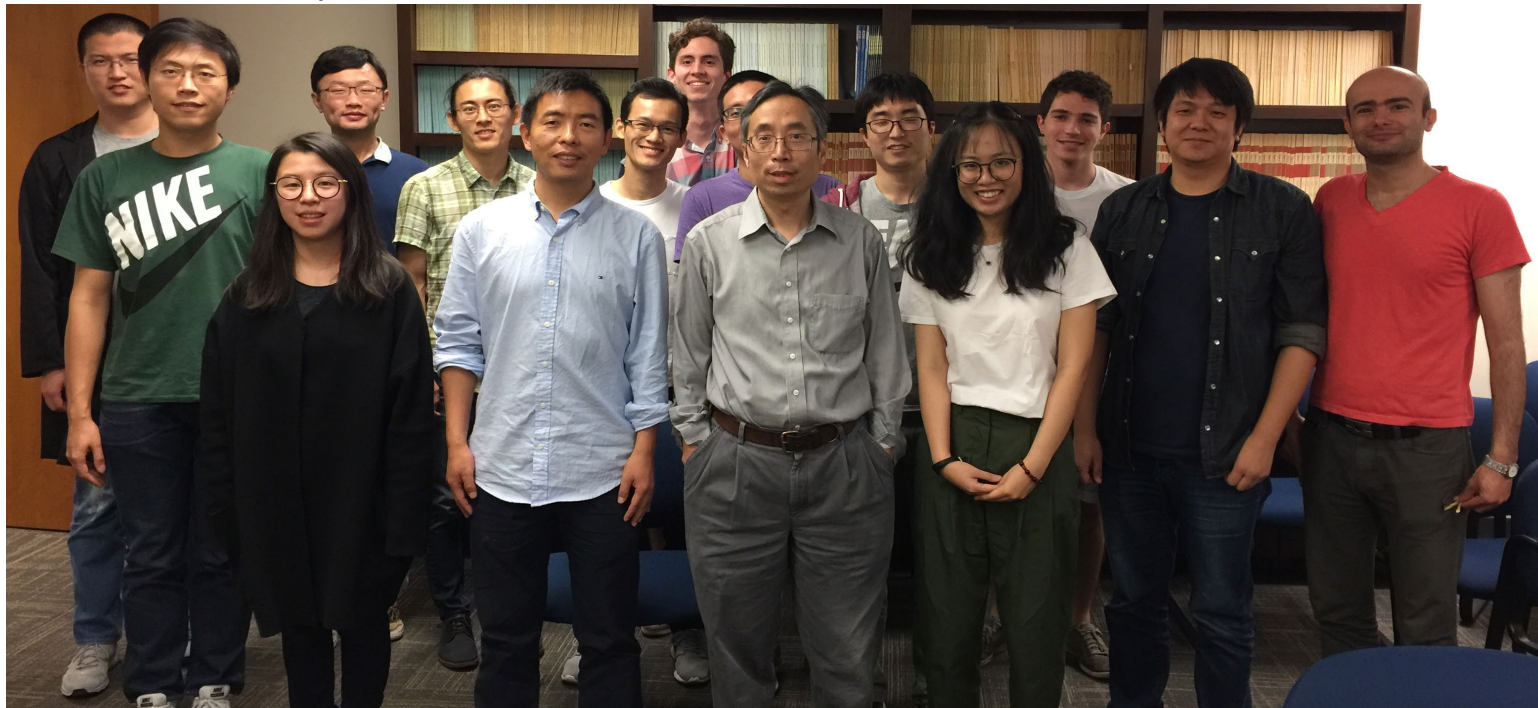
- Integration of multiscale and multi-modal medical data brings significant challenges for data sciences
- Multi-view deep learning offers a powerful way for heterogeneous data fusion while uncover their complex relationships
- The interpretability of multi-view deep learning is challenging but important towards biological discovery

*Weizheng Yan, et al., Deep learning in neuroimaging: promises and challenges, IEEE Signal Processing Magazine, March, 2022, in press.*

# Acknowledgments

- Alexj Gossman, Y. Bai, B. Cai, W. Hu, O. Richfield, M. Wang, J. Wang, A. Zhang, Tulane Univ.
- Keith Dillion, S.- P. Deng, Jian Fang, Pascal Zille, Ashad Alam, Tulane
- J. Duan, C. Qiao, XJTU, CHINA
- Vince Calhoun, GSU/Gatech/Emory
- Julia Stephen, Mind Research Network
- Tony Wilson, Boys Town National Hospital
- H. W. Deng, Tulane Global Biostatistics and Data Sciences

Funding sources: NIH(R01GM109068, R01MH104680,  
R01MH107354), and NSF#1539067



**Visit us at**  
<http://www.tulane.edu/~wyp>

Email: [wyp@tulane.edu](mailto:wyp@tulane.edu)



Finding needle in the haystack!